Facile Synthesis of a Cholesterol-Doxorubicin Conjugate Using Cholesteryl-4-Nitrophenolate as an Activated Ester and Biological Properties Analysis

Pedro Freitas , Dina Maciel , Jolanta Jaśkowska , Kamila Zeńczak-Tomera , Yanbiao Zhou , Guoyin Yin , Ruilong Sheng *

Posted Date: 19 November 2024

doi: 10.20944/preprints202411.1450.v1

Keywords: Cholesterol; doxorubicin; conjugate; 4-nitrophenolate; theoretical calculation

Article

Facile Synthesis of a Cholesterol-Doxorubicin Conjugate Using Cholesteryl-4-Nitrophenolate as an Activated Ester and Biological Properties Analysis

Pedro Freitas [1], Dina Maciel [1], Jolanta Jaśkowska [2], Kamila Zeńczak-Tomera [2], Yanbiao Zhou [3], Guoyin Yin [4] and Ruilong Sheng [1,*]

[1] CQM-Centro de Química da Madeira, MMRG, Universidade da Madeira, Campus da Penteada, 9020-105 Funchal, Portugal
[2] Cracow University of Technology, Faculty of Chemical Engineering and Technology, 24 Warszawska Street, 31-155 Cracow, Poland
[3] College of Chemistry and Environmental Engineering, Pingdingshan University, Pingdingshan 467000, Henan, China
[4] Analytical Department, STA Pharmaceutical US LLC, 6114 Nancy Ridge Drive, San Diego, CA 92121, United States
* Correspondence: ruilong.sheng@staff.uma.pt; Tel.: +351-2917-05254

Abstract: Developing new biomolecule-drug conjugates as prodrugs is a promising area for natural products and pharmaceutical chemistry. Herein, a cholesterol-doxorubicin (Chol-DOX) conjugate was synthesized using cholesteryl-4-nitrophenolate as a facile, stable, and controllable activated ester. This approach offers an alternative to the conventional HCl-emitting cholesteryl chloroformate method, semi-empirical theoretical calculations showed that cholesteryl-4-nitrophenolate exhibits moderate reactivity, higher thermodynamic stability, and a lower HOMO-LUMO energy gap compared to cholesteryl chloroformate, suggesting cholesteryl-4-nitrophenolate could be used as a more controllable acylating agent. The structure of synthesized Chol-DOX conjugate was characterized using NMR and MS techniques. Biological properties of the Chol-DOX were analyzed with the comparison of theoretical and experimental data. This work provided a facile and controllable method to synthesize natural lipid-DOX prodrug and offered an in-depth data analysis of the related biological properties.

Keywords: cholesterol; doxorubicin; conjugate; 4-nitrophenolate; theoretical calculation

1. Introduction

Doxorubicin (DOX, also known as Adriamycin) is an anthracycline with aglycone linked to an amino-sugar moiety (daunosamine), it has been employed as a chemotherapeutic drug for the treatment of solid tumors and malignancies.[1] DOX inhibits topoisomerase II (Topo II) by DNA intercalating and by reactive oxidative species (ROS)-associated apoptosis. Free DOX is highly toxic, and its pharmacodynamics are challenging to control. To mitigate toxic side effects of DOX, conjugating natural products to the daunosamine moiety has proven to be an effective strategy for diminishing toxicity, improving selectivity, and enhancing cellular uptake of the drugs [2]. Particularly, the conjugation of DOX with biocompatible natural lipids could bring about enhanced cellular uptake and controllable drug release properties.

As a natural steroid lipid, cholesterol played essential roles as a precursor to all steroid hormones and bile acids with outstanding bioavailability and biocompatibility, which allowed it as a potential sustainable building block for biomaterials [3–9]. The cholesterol conjugate of anti-cancer drugs endowed them with controllable, quantitative, and enhanced drug delivery features for constructing nano-chemotherapeutics. In our previous work, a cholesterol-doxorubicin conjugate based nanoprodrug with enhanced breast cancer inhibition was synthesized [10] using the cholesteryl-chloroformate as an acylating agent. Nevertheless, cholesteryl chloroformate is a highly reactive agent that could result in drawbacks such as low storage stability, lack of selectivity, and high toxicity. Particularly, it could emit very toxic HCl gas in a moist environment through hydrolysis. The

 doi:10.20944/preprints202411.1450.v1

drawbacks prompted us to develop another activated ester cholesteryl-4-nitrophenolate as an alternative acylating reagent with better stability and controllable reactivity.

In this work, the molecular parameters, electrostatic potential, and local electron density of carbonyl groups of the cholesteryl chloroformate and cholesteryl-4-nitrophenolate were first theoretically calculated by a semi-empirical method. In our experimental approach, the unstable, HCl-emitting cholesteryl chloroformate was converted to a more stable cholesteryl-4-nitrophenolate, which was then coupled with free DOX under the presence of organic base triethylamine (TEA) to facilely synthesize the Chol-DOX conjugate. The molecular structures of both synthesized cholesteryl-4-nitrophenolate intermediate and final product Chol-DOX were characterized. In addition, the theoretical and experimental biological properties of the Chol-DOX were analyzed and discussed.

2. Materials and Methods

2.1. Theoretical molecular parameter and molecular electrostatic potential analysis

Molecular parameters and molecular electrostatic potential (MEP) of the cholesteryl chloroformate and cholesteryl-4-nitrophenolate were calculated by WebMO online software [11], using semi-empirical Molecular Orbital PACkage (MOPAC, v22.1.1 Linux) and Parameterization Method (PM) [12].

2.2. Chemical synthesis experimental

2.2.1. Materials and methods for the synthesis

Cholesteryl chloroformate (98.0 %), 4-nitrophenol (98.0 %), doxorubicin hydrochloride (DOX·HCl, 99.0 %) and triethylamine (TEA, 99.0 %) were purchased from Sigma-Aldrich and used as received. Other reagents and solvents were analytical grades and used without further purification. Aluminum TLC Silica Gel 60 F254 Plates were purchased from Merck. ^{1}H NMR and ^{13}C NMR were measured on a Bruker Avance II+ UltraShield™ 400 Plus Ultra Long Hold NMR spectrometer (at room temperature, ^{1}H nuclei at 400 MHz and ^{13}C at 100 MHz). The mass spectrum with electrospray ionization technique (ESI-MS) was conducted on a Bruker Autoflex maX MALDI-TOF-Mass Spectrometer (MALDI-TOF-MS, negative ion mode) at Centro de Química da Madeira in University of Madeira.

2.2.2. Synthesis of Cholesteryl-4-nitrophenolate (IUPAC name: [(3S,10R,13R,14S,17R)-10,13-dimethyl-17-(6-methylheptan-2-yl)-2,3,4,7,8,9,11,12,14,15,16,17-dodecahydro-1H-cyclopenta[a]-phenanthren-3-yl] (4-nitrophenyl) carbonate)

Cholesteryl chloroformate (45 mg, 0.1 mmol) was dissolved in 5 mL tetrahydrofuran (THF) with TEA (15 mg, 0.15 mmol) and put inside a 50 mL flask, 4-nitrophenol (17 mg, 0.12 mmol) was dissolved in 1 mL THF and the solution was added dropwise into the cholesteryl chloroformate solution, the mixture was stirred at room temperature (r.t.) for 6 hours. The solvent THF was removed by rotavapor under reduced pressure, 5 mL of saturated citric acid solution was added to neutralize TEA, and then extracted with 20 mL $CHCl_3$. The crude product was further purified by flash column chromatography (ethyl acetate: hexane=1:5, v: v) to obtain the cholesteryl-4-nitrophenolate (39.3 mg, yield: 71.2%).

^{1}H NMR ($CDCl_3$, 400 MHz, δ in ppm) δ 8.26 (2H, Ar-H, $^{2}J_{ortho}$=12.0 Hz, nitrophenolate), 7.40 (2H, Ar-H, $^{2}J_{ortho}$=12.0 Hz, nitrophenolate), 5.42 (1H, -CH=, Chol), 4.60 (1H, COCH), 2.50 (2H, -CH_2-C=, Chol) 2.30-0.79 (38 H, Cholesterol skeleton), 0.68 (3H, -CH_3, Chol)

^{13}C NMR ($CDCl_3$, 100 MHz, δ in ppm) 155.79, 151.91, 145.42, 138.98, 125.41, 123.67, 121.93, 79.90, 56.81, 56.27, 50.11, 42.46, 39.84, 39.65, 38.00, 36.93, 36.69, 36.32, 35.93, 32.05, 31.97, 28.36, 28.16, 27.73, 24.42, 23.97, 22.96, 22.71, 21.19, 19.41, 18.86, 12.01

3.2.3. Synthesis of Chol-DOX conjugate (IUPAC name: [(3S,10R,13R,17R)-10,13-dimethyl-17-(6-methylheptan-2-yl)-2,3,4,7,8,9,11,12,14,15,16,17-dodecahydro-1H-cyclopenta[a]phenanthren-3-yl] N-[(2S,3S,4S,6R)-3-hydroxy-2-methyl-6-[[(1S,3S)-3,5,12-trihydroxy-3-(2-hydroxyacetyl)-10-methoxy-6,11-dioxo-2,4-dihydro-1H-tetracen-1-yl]oxy]oxan-4-yl]carbamate)

 doi:10.20944/preprints202411.1450.v1

24.4 mg of DOX·HCl (0.04 mol) were weighed and mixed with 0.5 mL of dimethyl sulfoxide (DMSO), 0.25 mL of methanol (MeOH) and 0.25 mL of TEA. Cholesteryl-4-nitrophenolate was dissolved in 0.5 mL of DMSO and 0.5 mL of THF and added dropwise into the DOX solution. Then the reaction mixture was stirred at 40 ℃ for 24 hours. The reaction was monitored using thin layer chromatography (TLC) silica plates, when the reaction was completed, the solvent THF was removed by rotavapor at 40 ℃ under reduce pressure, 5 mL of saturated citric acid solution was added to neutralize TEA, and then extracted with 20 mL $CHCl_3$, the crude product was further purified by flash column chromatography (MeOH: $CHCl_3$=1:10, v: v). The eluent was removed under reduced pressure to obtain the conjugate Chol-DOX as a dark-red powder (26.1 mg, yield: 68.3%).

^{1}H NMR ($CDCl_3$, 400 MHz, δ in ppm): δ 13.97 (1H, Ar-OH, DOX), 13.24 (1H, Ar-OH, DOX), 8.02 (1H,Ar-H, DOX), 7.78 (1H, Ar-H, DOX), 7.28 (1H, Ar-H, DOX), 5.50 (1H, CH_2-O(H), DOX), 5.29 (1H, -CHO(O)-, DOX) and 1H, -CH=, DOX), 5.11 (1H, Ar-C(O)HCH), 4.78 (2H, -CH_2CO, DOX), 4.58 (1H, OCOO-CH, Chol), 4.10 (3H, -OCH_3, DOX), 3.81 (1H, -CH-NH, DOX), 3.68 (1H, -CH-O-, DOX), 3.18 and 3.06 (2H, Ar-CH_2 (H_a and H_b), Dox), 2.23-0.74 (51 H, Chol and Dox skeletons), 0.63 (3H, -CH_3, Chol)

^{13}C NMR ($CDCl_3$, 100 MHz, δ in ppm): δ 214.6, 187.3, 186.86, 186.76, 161.22, 156.14, 155.46, 136.09, 135.61, 135.17, 133.74, 133.56, 122.63, 120.81, 120.03, 118.62, 111.78, 111.42, 69.86, 65.73, 62.29, 56.83, 56.27, 50.14, 42.45, 39.87, 39.65, 38.74, 38.57, 37.11, 37.06, 36.69, 36.64, 36.32, 35.93, 35.76, 34.01, 28.37, 28.15, 24.42, 23.97, 22.96, 22.70, 21.18, 19.46, 18.85, 17.03, 12.00.

MALDI-TOF-MS (negative ion mode): [Chol-DOX-H^+]$^-$ calculated: 954.50, found: 954.649.

3. Results and discussion

3.1. Theoretical analysis of molecular parameters

For nucleophilic reactions, the acyl group's activity was determined by the electron density of the sp^2-carbon atom of the active carbonyl, higher positive charge (electropositivity) tend to readily react with electron-rich (nucleophilic) groups (such as NH_2 and OH). Herein, the molecular parameters and molecular electrostatic potential (MEP) were calculated by the MOPAC (v22.1.1 Linux) with PM6 semi-empirical method using WebMO online software.[11] The electron density and charge distribution could be visually presented on the MEP of molecules. The various colors represented the different electrostatic potentials of atoms (Figure 1), cholesteryl-4-nitrophenolate has a much lower local positive charge on the carbonyl group (ϱ_{COPh}=+0.7277-0.3332=0.3945) than that of cholesteryl-chloroformate (ϱ_{COCl}=+0.2493+0.5256=+0.8049), suggesting its moderate and controllable reactivity [13]. Moreover, the positive charge of cholesteryl-chloroformate localized on both sp^2-carbon (+0.2493) and chloride (+0.5256) atoms, while the cholesteryl-4-nitrophenolate's phenol oxygen atom has a negatively charged oxygen atom (-0.3332) and the positive charge only localized on the sp^2-carbon(+0.7277), suggesting its less nucleophilic reactivity compared to that of cholesteryl-chloroformate. The controllable reactivity of cholesteryl-4-nitrophenolate could bring about higher storage stability under moisture, easier handling feature, and fewer side reactions, which might improve its applicability in cholesteryl lipid conjugation and biomaterial modification.

Preprints.org (www.preprints.org) | NOT PEER-REVIEWED | Posted: 19 November 2024 doi:10.20944/preprints202411.1450.v1

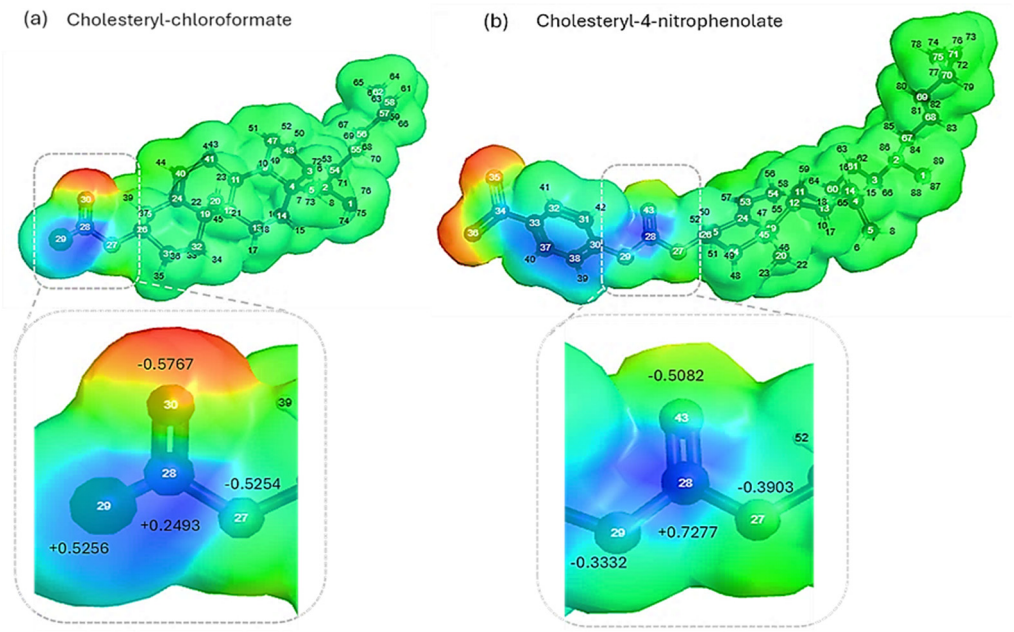

Figure 1. Molecular electrostatic potential (MEP) surfaces of the cholesteryl chloroformate (a) and cholesteryl-4-nitrophenolate (b) optimized structures were calculated by WebMO online software [11]. Red color: high electron density (electron-rich) region; blue color: low electron density (electron-poor) region; green/yellow color: neutral electrostatic region, magnified images of (a and b, bottom) showed the active carbonyl group regions labelled with calculated local electron density.

Theoretical molecular parameters of the cholesteryl-chloroformate and cholesteryl-4-nitrophenolate were also calculated using WebMO online software from the optimized structures, the data were shown in Table 1. Cholesteryl-4-nitrophenolate has significantly higher heat of formation (469.093 Kcal/mol) compared to cholesteryl-chloroformate (98.164 Kcal/mol), suggesting its greater thermodynamic stability. The large HOMO-LUMO gap for cholesteryl-chloroformate (9.000 eV) indicated its low light absorption capability, in contrast, the very small HOMO-LUMO gap of cholesteryl-4-nitrophenolate (0.134 eV) suggested its light absorption property, which is attributed to its aromatic 4-nitrophenolate structure. Moreover, cholesteryl-4-nitrophenolate has a much higher dipole moment (10.721 Debye), which indicates its stronger polarity and could easily interact with amphiphilic molecules or polar solvents [14].

Table 1. Comparison of the theoretical molecular properties of cholesteryl-chloroformate and cholesteryl-4-nitrophenolate calculated by WebMO software.

Molecular parameters	Cholesteryl-chloroformate	Cholesteryl-4-nitrophenolate
Molecular formula	$C_{28}H_{45}O_2Cl$	$C_{34}H_{49}NO_5$
Molecular weight (MW)	449.115	551.765
Heat of formation (Kcal/mol)	98.164	469.093
Molecular area (Å^2)	465.440	576.180
Molecular volume (Å^2)	595.540	713.880
LUMO energy (E_{LUMO}, eV)	+0.088	-12.812
HOMO energy (E_{HOMO}, eV)	-9.000	-13.946
HOMO-LUMO energy gap ($\Delta E = E_{LUMO}$-E_{HOMO}, eV)	9.088	0.134
Dipole moment (Debye)	2.855	10.721

3.2. Synthesis and characterization of Chol-DOX conjugate

First, the cholesteryl chloroformate was reacted with 4-nitrophenol to prepare cholesteryl-4-nitrophenolate using TEA as a catalyst [15,16], which was also a proton scavenger to absorb HCl

 doi:10.20944/preprints202411.1450.v1

released from the chloroformate. The reaction proceeded at room temperature for 6 h (Figure 2). Then the solvent was removed, and the TEA residue was neutralized with citric acid, the product was purified via silica gel flash column chromatography (ethyl acetate: hexane= 1:5, v: v) with a yield of 71.2%. For the facile and efficient synthesis of Chol-DOX conjugates, it is essential to use an organic base to catalyze the amide bond formation (amidation) under mild conditions. TEA was employed as a catalyst and proton scavenger in the reaction, which could convert the hydrochloride form of DOX into neutralized free DOX. Pyridine (PY) was widely used as a catalyst and/or solvent [17], while the PY-catalyzed amidation proceeded at slower rate and complex purification steps was required, which might be due to the hydrogen-bonding or π-π stacking interactions between pyridine and DOX and resulted in the formation of some complexes. Compared to PY, the TEA is a more efficient basic catalyst. Moreover, excessive TEA catalyst in the reaction mixture were much easier to be removed under vacuum distillation (Boiling point: ~ 40 ℃ at 0.15 atm.) [18,19]. After purification by silica gel flash column chromatography (MeOH: $CHCl_3$=1:10, v: v), the synthesized Chol-DOX conjugate was obtained as dark red solid powder with a yield of 68.3%.

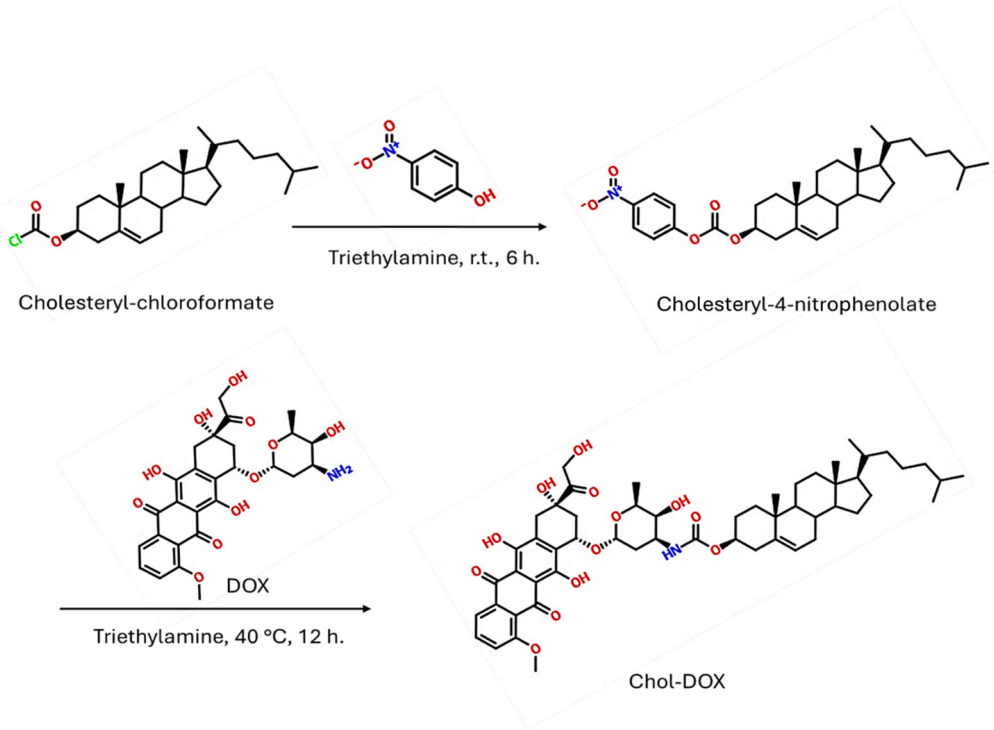

Figure 2. Synthesis of the cholesteryl-4-nitrophenolate activated ester, which was then coupled with DOX via aminolysis to synthesize Chol-DOX conjugate.

The ^{1}H and ^{13}C NMR spectra of the cholesteryl-4-nitrophenolate activated ester were shown in Figure S1 (supporting information). The proton signals of nitrophenolate were found at δ 8.26 ppm and δ 7.40 ppm, with a strong ortho H-H coupling constant ($^2J_{ortho}$=12.0 Hz). The signal at δ 5.42 ppm and δ 4.60 ppm were identified as the double-bond (alkenyl) proton (-C=CH-) of the cholesteryl moiety and the proton attached to the carbonate (-OCOO-) group, respectively. In the ^{13}C NMR, the chemical shift of carbon atom on the carbonyl group (-C=O) was observed at δ 155.79 ppm. The carbon signals of nitrophenolate ring were observed at δ 151.9, 145.42, 125.41 and 121.93 ppm. The double-bond (alkenyl) carbon atoms (-C=CH-) of the cholesteryl moiety were detected at δ 138.98 and 123.67 ppm. The signal at δ 79.90 ppm was identified as the carbon atom on the cholesteryl moiety attached to the oxygen of carbonate (-OCOO-CH) group.

The ^{1}H and ^{13}C NMR spectra of the synthesized Chol-DOX conjugate were shown in Figure 3. For the ^{1}H NMR spectrum, the proton signals in the range of δ 7.28-7.41 ppm were identified as the aromatic protons (-ArH). The signals at δ 13.97 and 13.21 ppm were attributed as hydroxyl groups (-OH), and δ 4.10 ppm belongs to the methoxy group (-OCH_3) on the DOX moiety. The alkenyl proton (-C=CH-) appeared at δ 5.28 ppm. Moreover, aliphatic proton signals (δ 0.63 to 2.41 ppm) on the cholesteryl backbone/skeleton could be clearly observed. For the ^{13}C NMR spectrum, δ 214.6 ppm and

 doi:10.20944/preprints202411.1450.v1

187.3 ppm were assigned as the signals of the carbonyl carbon atoms in the conjugate. δ 161.22 ppm and 156.14 ppm are identified as the signals of the aromatic carbons of the DOX. The Chol-DOX structure was confirmed by identifying the carbon signals of the carbonyl groups, aromatic carbons, and the cholesteryl backbone/skeleton (various carbon signals in the range of δ 69.86 ppm to 12.00 ppm). Moreover, the MALDI-TOF-MS spectrum showed a molecular negative ion peak at m/z 954.649, which was very close to the calculated value 954.50 for the deprotonated Chol-DOX conjugate ([Chol-DOX-H^+]$^-$). The ^{1}H NMR, ^{13}C NMR and MALDI-TOF-MS results confirmed the successful preparation of the Chol-DOX conjugate.

The synthesized Chol-DOX appeared as a dark-red solid powder (Figure S2a, supporting information), the solid-state indicated that it could be conveniently handled and stored. When the Chol-DOX conjugate solid powder was added into PBS (0.1 M) solution, the precipitates of Chol-DOX could be clearly observed, indicating Chol-DOX has poor-solubility (almost insoluble) in water or under an aqueous environment. (Figure S2b, supporting information) The poor-solubility was due to the conjugation of a strong hydrophobic cholesteryl moiety to the amphiphilic DOX. Thin-layer chromatography (TLC) plate analysis of the Chol-DOX showed a high R_f value (0.85) and low polarity (Figure S2c), which further suggested that the introduction of cholesteryl moiety could significantly reduce the polarity of DOX. The low polarity of Chol-DOX (calculated LogP value: 8.57) could benefit higher cell membrane permeability and enhance cellular uptake efficiency, which might change its pharmacokinetics and intracellular behaviors.

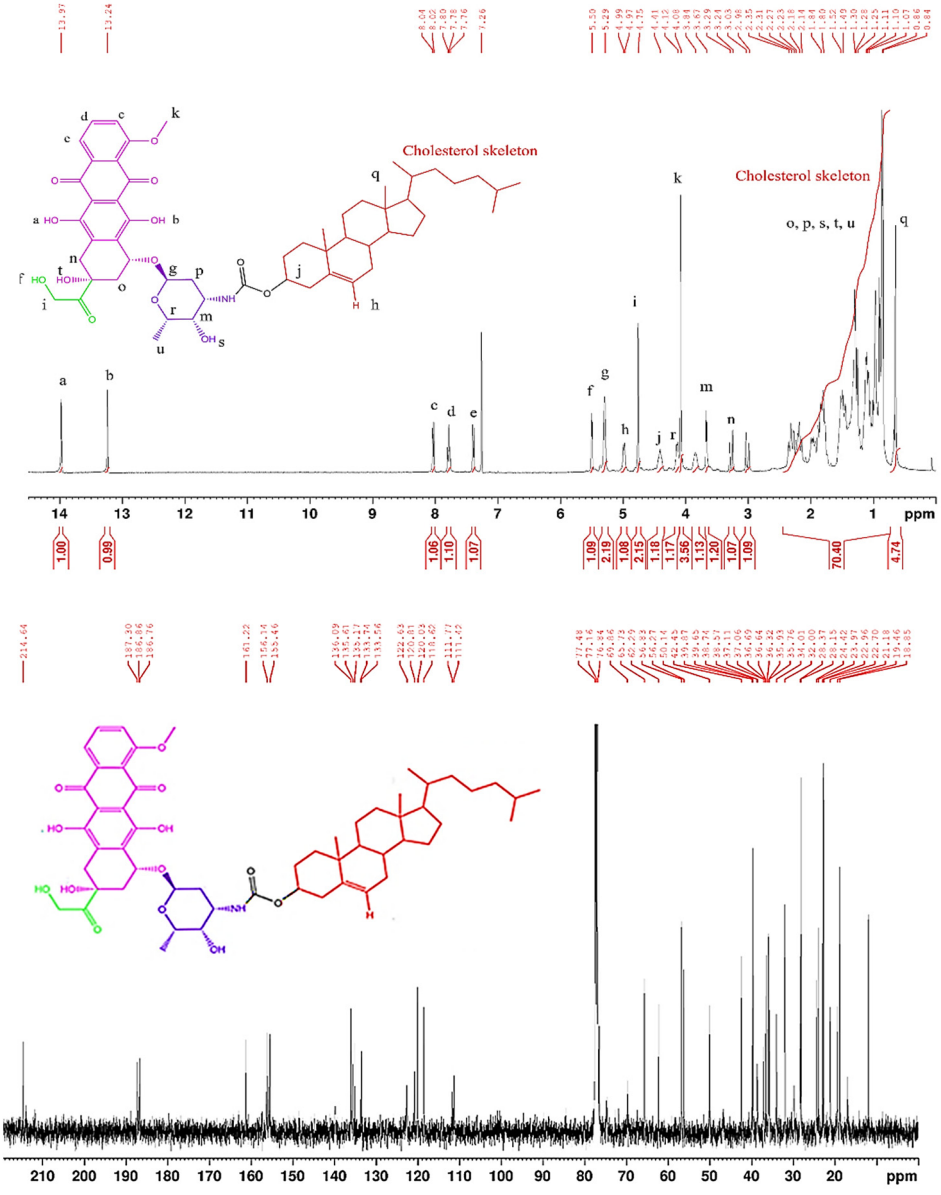

 doi:10.20944/preprints202411.1450.v1

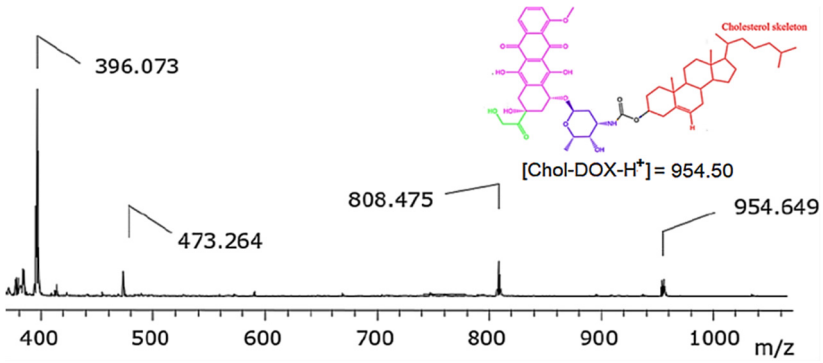

Figure 3. Top to bottom: the original ^{1}H NMR ($CDCl_3$, 400 MHz), ^{13}C NMR ($CDCl_3$, 100 MHz) and MALDI-TOF-MS (negative ion mode) spectra of the synthesized Chol-DOX conjugate.

Theoretical (predicted on the SwissADME software [20,21]) and experimental data analysis were conducted to explore the biological properties of the Chol-DOX conjugate using free DOX as the control. As shown in Table 2, both free DOX and Chol-DOX exhibited low gastrointestinal (GI) absorption and blood brain barrier (BBB) penetration capability due to their potential as the substrates for P-glycoprotein (P-gp). Both Chol-DOX and free DOX have no inhibitory effects on cytochrome P450 (CYP) enzymes CYP1A2, CYP2C19, and CYP2D6, which could reduce their CYP-catalyzed drug degradation. The inhibition of CYP3A4 might increase their plasma levels. Notably, Chol-DOX demonstrated a significantly improved octane-water partition coefficient (Log $P_{o/w}$=5.80) than free DOX (Log $P_{o/w}$=2.58), implying its higher hydrophobicity (or lipophilicity) [22]. This property was beneficial to improve the cell membrane permeability and to increase the cellular uptake efficiency of Chol-DOX.

Table 2. Theoretical and experimental biological properties (pharmacokinetics, druglikeness, cell inhibition efficacy and localization) of the free DOX and Chol-DOX conjugate.

Biological Properties	Free DOX	Chol-DOX
GI absorption [a]	Low	Low
BBB permeant [a]	No	No
P-gp substrate [a]	Yes	Yes
CYP1A2 inhibitor [a]	No	No
CYP2C19 inhibitor [a]	No	No
CYP2C9 inhibitor [a]	No	No
CYP2D6 inhibitor [a]	No	No
CYP3A4 inhibitor [a]	Yes	Yes
Log K_p (skin permeation, cm/s) [a]	-8.71	-4.37
Log $P_{o/w}$ (iLOGP) [a]	2.58	5.80
Lipinski Druglikeness [a]	No (3 violations): MW>500; number of N or O atoms >10; NH or OH groups >5)	No (3 violations): MW>500, number of N or O atoms >10, NH or OH groups >5
Bioavailability Score [a]	0.17	0.17
MDA-MB-231 cell viability (%) with 2, 6, 10ug/mL DOX, respectively.[b]	87.1, 74.3, 70.2	98.9, 94.3, 82.1
MCF-7 cell viability (%) with 2, 6, 10ug/mL DOX, respectively.[b]	67.3, 64.1, 60.7	95.9, 79.4, 62.4
Intracellular localization [b]	cell nuclei	lysosome

[a] the theoretical data were calculated on the SwissADME online software; [b] the experimental/tested data were cited from our previous research work [10] .

 doi:10.20944/preprints202411.1450.v1

The experimental data revealed that the Chol-DOX have obviously lower breast cancer cytotoxicity in MDA-MB-231 (98.9%, 94.3%, 82.1% cell viability for 2, 6, and 10 μg/mL, respectively) and MCF-7 cell lines (95.9%, 79.4%, 62.4% for the same concentrations), compared to that of free DOX (87.1%, 74.3%, 70.2% cell viability for MDA-MB-231 and 67.3%, 64.1%, 60.7% for MCF-7 cells), which might be due to the 'endosome-lysosome-autophagosome encapsulation process' of Chol-DOX and the slow acidic hydrolysis of its carbonate linkage. Interestingly, the intracellular localization of Chol-DOX in lysosomes instead of cell nuclei (free DOX mainly localized in cell nuclei after 12 h incubation) implied a more controllable drug delivery mechanism of Chol-DOX [10]. The bioavailability radar plots (Figure 5) of free DOX and Chol-DOX (predicted by SwissADME software [23]) also demonstrated their significant difference. This profile suggested that Chol-DOX has more limitations on the absorption, distribution, metabolism, and excretion properties compared to free DOX, it was suitable to serve as a prodrug rather than a 'direct' drug. In addition, the biological properties indicated that the Chol-DOX conjugate might be employed as a more controllable alternative to free DOX. Further study on optimizing the Chol-DOX's bioavailability and anti-cancer efficacy is undergoing in our lab.

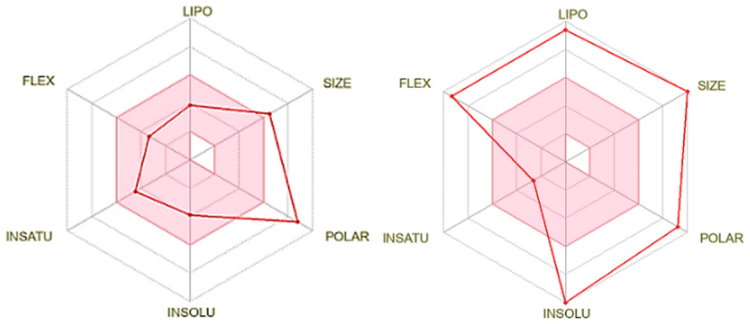

Figure 4. The bioavailability radar plots of DOX (left) and Chol-DOX (right) predicted by SwissADME online software. (LIPO: lipophilicity, SIZE: molecular size (weight), POLAR: molecular polarity, INSOLU: water insolubility, INSATU: molecular unsaturation, FLEX: molecular rotatable bond flexibility).

4. Conclusions

In summary, we synthesized a cholesterol-doxorubicin conjugate using a stable cholesteryl-4-nitrophenolate ester, which could be employed as a more controllable and safer alternative to the unstable, HCl-emitting cholesteryl-chloroformate. The theoretical calculations indicated that cholesteryl-4-nitrophenolate exhibited high thermodynamic stability, moderate reactivity, higher dipole moment and a small HOMO-LUMO gap. The synthesized Chol-DOX conjugate was fully characterized using NMR and MS techniques. The synthesized Chol-DOX conjugate demonstrated high lipophilicity and low water solubility, which may improve its cell membrane permeability and enhance therapeutic efficiency. This work provided a controllable method to synthesize Chol-DOX and offered an in-depth analysis of its biological properties.

Supplementary Materials: The following supporting information can be downloaded at: www.mdpi.com/xxx/s1.

Author Contributions: The individual contributions were provided as: Conceptualization, R. S.; methodology, P. F., D. M.; software, D. M., R. S.; validation, J. J., K. Z., Y. Z., G. Y.; formal analysis, D. M., J. J., K. M., Y. Z., G. Y.; investigation, P. F., D. M., R. S.; resources, R. S.; data curation, P. F.; writing—original draft preparation, P. F., R. S.; writing—review and editing, D. M., J. J., K. M., Y. Z., G. Y., R. S.; visualization, P. F., D. M., R. S.; supervision, D. M., R. S.; project administration, R. S., D. M.; funding acquisition, R. S., D. M. All authors have read and agreed to the published version of the manuscript.

Funding: Please add: This research was supported by FCT-Fundação para a Ciência e a Tecnologia through the CQM Base Fund-UIDB/00674/2020 and Programmatic Fund-UIDP/00674/2020. Dr. Ruilong Sheng thanks the FCT-individual employment grant 2021.00453. CEECIND. Dr. Dina Maciel appreciates Secretaria Regional da Educação, Ciência e Tecnologia e a Agência Regional para o Desenvolvimento da Investigação, Tecnologia e Inovação (ARDITI) for the support..

Data Availability Statement: We encourage all authors of articles published in MDPI journals to share their research data. In this section, please provide details regarding where data supporting reported results can be

found, including links to publicly archived datasets analyzed or generated during the study. Where no new data were created, or where data is unavailable due to privacy or ethical restrictions, a statement is still required. Suggested Data Availability Statements are available in section "MDPI Research Data Policies" at https://www.mdpi.com/ethics.

Acknowledgments: This research was supported by FCT-Fundação para a Ciência e a Tecnologia through the CQM Base Fund-UIDB/00674/2020 (DOI: 10.54499/UIDB/00674/2020) and Programmatic Fund-UIDP/00674/2020 (DOI 10.54499/UIDP/00674/2020). Dr. Ruilong Sheng thanks the FCT-individual employment grant 2021.00453. CEECIND. Dr. Dina Maciel appreciates Secretaria Regional da Educação, Ciência e Tecnologia e a Agência Regional para o Desenvolvimento da Investigação, Tecnologia e Inovação (ARDITI) for the support.

Conflicts of Interest: The authors declare no conflicts of interest.

References

1. Sritharan, S.; Sivalingam, N. A comprehensive review on time-tested anticancer drug doxorubicin. *Life Sciences* **2021**, *278*, 119527, doi:https://doi.org/10.1016/j.lfs.2021.119527.
2. Gonçalves, M.; Mignani, S.; Rodrigues, J.; Tomás, H. A glance over doxorubicin based-nanotherapeutics: From proof-of-concept studies to solutions in the market. *Journal of Controlled Release* **2020**, *317*, 347-374, doi:https://doi.org/10.1016/j.jconrel.2019.11.016.
3. Wang, Z.; Luo, T.; Cao, A.; Sun, J.; Jia, L.; Sheng, R. Morphology-Variable Aggregates Prepared from Cholesterol-Containing Amphiphilic Glycopolymers: Their Protein Recognition/Adsorption and Drug Delivery Applications. *Nanomaterials* **2018**, *8*, 136, doi:10.3390/nano8030136.
4. Sheng, R.; Wang, Z.; Luo, T.; Cao, A.; Sun, J.; Kinsella, J.M. Skeleton-Controlled pDNA Delivery of Renewable Steroid-Based Cationic Lipids, the Endocytosis Pathway Analysis and Intracellular Localization. *International Journal of Molecular Sciences* **2018**, *19*, 369, doi:10.3390/ijms19020369.
5. Sheng, R.; Luo, T.; Li, H.; Sun, J.; Wang, Z.; Cao, A. Cholesterol-based cationic lipids for gene delivery: Contribution of molecular structure factors to physico-chemical and biological properties. *Colloids and Surfaces B: Biointerfaces* **2014**, *116*, 32-40, doi:10.1016/j.colsurfb.2013.12.039.
6. Wang, Z.; Sun, J.; Li, M.; Luo, T.; Shen, Y.; Cao, A.; Sheng, R. Natural steroid-based cationic copolymers cholesterol/diosgenin-r-PDMAEMAs and their pDNA nanoplexes: impact of steroid structures and hydrophobic/hydrophilic ratios on pDNA delivery. *RSC Advances* **2021**, *11*, 19450-19460, doi:10.1039/D1RA00223F.
7. Zhu, Z.; Zhang, L.; Sheng, R.; Chen, J. Microfluidic-Based Cationic Cholesterol Lipid siRNA Delivery Nanosystem: Highly Efficient In Vitro Gene Silencing and the Intracellular Behavior. *International Journal of Molecular Sciences* **2022**, *23*, 3999, doi:10.3390/ijms23073999.
8. Wang, Z.; Song, W.; Sheng, R.; Guo, X.; Hao, L.; Zhang, X. Controlled preparation of cholesterol-bearing polycations with pendent l-lysine for efficient gene delivery. *International Journal of Polymeric Materials and Polymeric Biomaterials* **2023**, *72*, 750-758, doi:10.1080/00914037.2022.2058943.
9. Wang, Z.; Guo, X.; Hao, L.; Zhang, X.; Lin, Q.; Sheng, R. Charge-Convertible and Reduction-Sensitive Cholesterol-Containing Amphiphilic Copolymers for Improved Doxorubicin Delivery. *Materials* **2022**, *15*, 6476, doi:10.3390/ma15186476.
10. Olim, F.; Neves, A.R.; Vieira, M.; Tomás, H.; Sheng, R. Self-Assembly of Cholesterol-Doxorubicin and TPGS into Prodrug-Based Nanoparticles with Enhanced Cellular Uptake and Lysosome-Dependent Pathway in Breast Cancer Cells. *European Journal of Lipid Science and Technology* **2021**, *123*, 2000337, doi:https://doi.org/10.1002/ejlt.202000337.
11. Polik, W.F.; Schmidt, J.R. WebMO: Web-based computational chemistry calculations in education and research. *WIREs Computational Molecular Science* **2022**, *12*, e1554, doi:https://doi.org/10.1002/wcms.1554.
12. Amić, A.; Gotal, E. Selected Thermodynamic Parameters of Antioxidant Activity of Coumarin Based Heterocyclic Compounds. *Chemistry Proceedings* **2021**, *3*, doi:10.3390/ecsoc-24-08385.
13. Lu, J.; Paci, I.; Leitch, D.C. A broadly applicable quantitative relative reactivity model for nucleophilic aromatic substitution (SNAr) using simple descriptors. *Chemical Science* **2022**, *13*, 12681-12695, doi:10.1039/D2SC04041G.
14. Darvishmanesh, S.; Vanneste, J.; Tocci, E.; Jansen, J.C.; Tasselli, F.; Degrève, J.; Drioli, E.; Van der Bruggen, B. Physicochemical Characterization of Solute Retention in Solvent Resistant Nanofiltration: the Effect of Solute Size, Polarity, Dipole Moment, and Solubility Parameter. *The Journal of Physical Chemistry B* **2011**, *115*, 14507-14517, doi:10.1021/jp207569m.
15. Brahmachari, G.; Nayek, N.; Nurjamal, K.; Karmakar, I.; Begam, S. Triethylamine — A Versatile Organocatalyst in Organic Transformations: A Decade Update. *Synthesis* **2018**, *50*, 4145-4164, doi:10.1055/s-0037-1609909.
16. Cai, L.; Wang, S. Elucidating Colorization in the Functionalization of Hydroxyl-Containing Polymers Using Unsaturated Anhydrides/Acyl Chlorides in the Presence of Triethylamine. *Biomacromolecules* **2010**, *11*, 304-307, doi:10.1021/bm901237t.

17. Fu, Z.; Zhang, L.; Hang, S.; Wang, S.; Li, N.; Sun, X.; Wang, Z.; Sheng, R.; Wang, F.; Wu, W.; et al. Synthesis of Coumarin Derivatives: A New Class of Coumarin-Based G Protein-Coupled Receptor Activators and Inhibitors. *Polymers* **2022**, *14*, doi:10.3390/polym14102021.
18. Grolier, J.P.E.; Roux-Desgranges, G.; Berkane, M.; Jiménez, E.; Wilhelm, E. Heat capacities and densities of mixtures of very polar substances 2. Mixtures containing N, N-dimethylformamide. *The Journal of Chemical Thermodynamics* **1993**, *25*, 41-50, doi:https://doi.org/10.1006/jcht.1993.1005.
19. Mokbel, I.; Razzouk, A.; Sawaya, T.; Jose, J. Experimental Vapor Pressures of 2-Phenylethylamine, Benzylamine, Triethylamine, and cis-2,6-Dimethylpiperidine in the Range between 0.2 Pa and 75 kPa. *Journal of Chemical & Engineering Data* **2009**, *54*, 819-822, doi:10.1021/je800603z.
20. Bakchi, B.; Krishna, A.D.; Sreecharan, E.; Ganesh, V.B.J.; Niharika, M.; Maharshi, S.; Puttagunta, S.B.; Sigalapalli, D.K.; Bhandare, R.R.; Shaik, A.B. An overview on applications of SwissADME web tool in the design and development of anticancer, antitubercular and antimicrobial agents: A medicinal chemist's perspective. *Journal of Molecular Structure* **2022**, *1259*, 132712, doi:https://doi.org/10.1016/j.molstruc.2022.132712.
21. Daina, A.; Michielin, O.; Zoete, V. SwissADME: a free web tool to evaluate pharmacokinetics, drug-likeness and medicinal chemistry friendliness of small molecules. *Scientific Reports* **2017**, *7*, 42717, doi:10.1038/srep42717.
22. Han, S.; Mei, L.; Quach, T.; Porter, C.; Trevaskis, N. Lipophilic Conjugates of Drugs: A Tool to Improve Drug Pharmacokinetic and Therapeutic Profiles. *Pharmaceutical Research* **2021**, *38*, 1497-1518, doi:10.1007/s11095-021-03093-x.
23. Chaves-Carballo, K.; Lamoureux, G.V.; Perez, A.L.; Bella Cruz, A.; Cechinel Filho, V. Novel one-pot synthesis of a library of 2-aryloxy-1,4-naphthoquinone derivatives. Determination of antifungal and antibacterial activity. *RSC Advances* **2022**, *12*, 18507-18523, doi:10.1039/D2RA01814D.